

## Charmless $b$ -hadron decays

G. DUJANY<sup>(\*)</sup>

*The University of Manchester - Manchester, UK*

received 16 September 2017

**Summary.** — Six recent LHCb results in the field of charmless  $b$ -hadron decays are presented: the first observation of a  $B_s^0$  baryon decay, the first observation of three new  $B_{(s)}^0 \rightarrow p\bar{p}h^+h'^-$  decay modes—where  $h$  and  $h'$  each denote a kaon or a pion—and the evidence of a fourth one, the first observation of the decay  $B^0 \rightarrow K^+K^-$ —the rarest hadronic  $B$  decay ever observed—and the first evidence of  $CP$  violation in baryon decays and in the  $B_s^0 \rightarrow K^+K^-$  decay.

### 1. – Introduction

Charmless  $b$ -hadron decays are a unique laboratory to probe  $CP$  violation and to look for new physics. These decays often proceed via a  $b \rightarrow u$  transition, dominated by tree-level Feynman diagrams, and  $b \rightarrow s$  and  $b \rightarrow d$  transitions, dominated by penguin loop diagrams. Due to the small magnitude of the  $V_{ub}$  Cabibbo-Kobayashi-Maskawa (CKM) matrix element, tree and penguin diagrams can have similar magnitude and their interference is sensitive to weak phases. Moreover beyond the Standard Model particles could produce sizeable differences with respect to the Standard Model expectations, both in the branching fractions and in the amount of  $CP$  violation, by entering as virtual particles in the loops of the penguin diagrams. Finally studying charmless  $b$ -hadron decays provides vital inputs and stringent tests for quantum chromodynamics (QCD) models.

In this proceedings six recent results by the LHCb Collaboration in the field of charmless  $b$ -hadron decays are described. The LHCb detector is a single-arm forward spectrometer covering the pseudorapidity range  $2 < \eta < 5$ , described in detail in refs. [1,2]. During Run I, it collected an integrated luminosity of approximately  $3 \text{ fb}^{-1}$ , of which  $1 \text{ fb}^{-1}$  was gathered at  $\sqrt{s} = 7 \text{ TeV}$  and  $2 \text{ fb}^{-1}$  at  $\sqrt{s} = 8 \text{ TeV}$ ; all the analyses described in the following sections have been performed using this dataset. The inclusion of charge-conjugation is implied throughout this document.

---

<sup>(\*)</sup> On behalf of the LHCb Collaboration.

## 2. – Baryonic $B$ decays

Due to their large mass,  $B$  mesons can also decay to baryons however many such decays have still to be observed. The first observation of a baryonic  $B$ -meson decay was done in 2002 by the Belle Collaboration [3] followed by the observation of several other baryonic decays of  $B^0$  and  $B^+$  mesons [4]. The first observation of a baryonic  $B_c^+$  decay was made by the LHCb Collaboration in 2014 [5], together with the first evidence of  $CP$  violation in a baryonic  $B$  decay [6]. The first observation of a baryonic  $B_s^0$  decay, the last of the four  $B$  meson species for which a baryonic decay mode had yet to be observed, is reported in the next sections.

In contrast to their mesonic counterparts, two-body baryonic decays are more rare than multibody ones: the typical branching fraction of a  $B$  meson decaying into a charmless baryon-antibaryon pair is around  $10^{-8}$ – $10^{-7}$ , while if a meson is also produced the branching fraction is  $\mathcal{O}(10^{-6})$ . The only two-body baryonic  $B$  meson decay observed to date is  $B^0 \rightarrow p\bar{\Lambda}(1520)$  [7] while evidence has been obtained for  $B^0 \rightarrow p\bar{p}$  [8] and  $B^0 \rightarrow p\bar{\Lambda}$  [9]. Another interesting phenomenon is the threshold enhancement observed in the lower region of the baryon-antibaryon mass spectrum in many multibody baryonic  $B$  decays. This phenomenon was first seen in  $B^+ \rightarrow p\bar{p}K^+$  [3] and  $B \rightarrow p\bar{p}D^{(*)}$  [10] and observed in other three-body  $B$ -meson decays [4] including decays with a baryon-antibaryon pair different from  $p\bar{p}$  like  $B^0 \rightarrow p\bar{\Lambda}\pi^-$  [11] and  $B^+ \rightarrow \Lambda\bar{\Lambda}K^+$  [12].

**2.1. Observation of the  $B_s^0 \rightarrow p\bar{\Lambda}K^-$  decay.** – As three body baryonic decays have larger branching fractions than two body ones  $B_s^0 \rightarrow p\bar{\Lambda}K^-$  is a natural candidate for the first observation of a baryonic  $B_s^0$  decay [13]. The decay  $B^0 \rightarrow p\bar{\Lambda}\pi^-$  is used as normalisation mode. Candidates are selected in a similar way for both the signal and the normalisation decay. Each  $B_s^0$  ( $B^0$ ) candidate is reconstructed by combining a proton and a kaon (pion) candidate with a  $\bar{\Lambda}$  candidate, reconstructed from the  $\bar{\Lambda} \rightarrow \bar{p}\pi^+$  decay. Two different reconstruction categories are used depending if the  $\bar{\Lambda}$  decays early enough for its daughters to be reconstructed in the VELO or not. The first reconstruction category has better mass, momentum and vertex resolution than the second one. Both the  $B_s^0 \rightarrow p\bar{\Lambda}K^-$  and the  $B^0 \rightarrow p\bar{\Lambda}\pi^-$  decay chains are refitted [14] employing a mass constraint on the  $\bar{\Lambda}$  candidates. Backgrounds from the  $B^0 \rightarrow \bar{\Lambda}_c^- p$  decay with  $\bar{\Lambda}_c^- \rightarrow \bar{\Lambda}\pi$  ( $\bar{\Lambda}_c^- \rightarrow \bar{\Lambda}K$ ) are removed with a veto around the  $\Lambda_c^+$  mass [15]. To separate the signal from the combinatorial background a multilayer perceptron [16] is used for each year of data taking and reconstruction category. Particle identification (PID) requirements are applied on the meson not coming from the  $\bar{\Lambda}$  decay to separate the signal from the normalisation mode. The sample is divided into eight mutually exclusive subsamples, according to the year of data taking, the  $\bar{\Lambda}$  reconstruction category and the final-state hypothesis. The yields of the signals as well as that of the normalisation mode are extracted with a simultaneous unbinned extended maximum likelihood fit to the invariant mass distributions of these eight subsamples. Each fit contains components for both  $B_s^0 \rightarrow p\bar{\Lambda}K^-$  and  $B^0 \rightarrow p\bar{\Lambda}\pi^-$  as well for the combinatorial background and the peaking backgrounds  $B_s^0 \rightarrow p\bar{\Sigma}K^-$  and  $B^0 \rightarrow p\bar{\Sigma}\pi^-$ . The fit projection for one subsample is shown in fig. 1 together with the background subtracted [17]  $p\bar{\Lambda}$  mass distribution for the  $B_s^0 \rightarrow p\bar{\Lambda}K^-$  decay where the threshold enhancement is clearly visible. The decay  $B_s^0 \rightarrow p\bar{\Lambda}K^-$  is observed with a statistical significance greater than 15 standard deviations ( $\sigma$ ) and its branching fraction is measured to be

$$\mathcal{B}(B_s^0 \rightarrow p\bar{\Lambda}K^-) + \mathcal{B}(\bar{B}_s^0 \rightarrow p\bar{\Lambda}K^-) = (5.48_{-0.80}^{+0.82} \pm 0.60 \pm 0.51 \pm 0.32) \times 10^{-6},$$

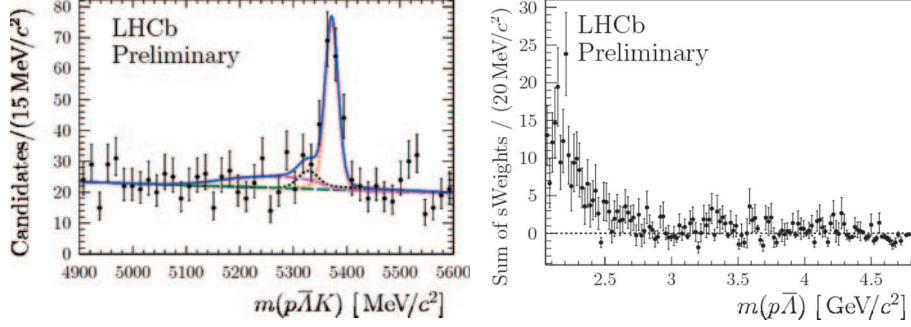


Fig. 1. – (Left) Result of the fit to the  $B_s^0 \rightarrow p\bar{\Lambda}K^-$  decay for the 2012 data sample with the  $\bar{\Lambda}$  decaying outside the VELO. The black points represent the data, the solid blue curve the complete fit model, the red (black) dotted curve the  $B_s^0 \rightarrow p\bar{\Lambda}K^-$  ( $B^0 \rightarrow p\bar{\Lambda}\pi^-$ ) contribution and the green (magenta) dashed curve the contribution from  $B^0 \rightarrow p\bar{\Sigma}\pi^-$  ( $B_s^0 \rightarrow p\bar{\Sigma}K^-$ ). (Right) Background subtracted [17]  $p\bar{\Lambda}$  mass distribution for the  $B_s^0 \rightarrow p\bar{\Lambda}K^-$  decay. Reproduced from [13].

where the first uncertainty is statistical, the second systematic, the third comes from the uncertainty on the branching fraction of the normalisation mode and the fourth from the uncertainty on the ratio of  $b$ -quark hadronisation probabilities ( $f_d/f_s$ ).

**2.2. Observation of the  $B_{(s)}^0 \rightarrow p\bar{p}h^+h'^-$  decays.** – Decays of  $B^0$  and  $B_s^0$  mesons to the charmless baryonic final states  $p\bar{p}h^+h'^-$ , where  $h$  and  $h'$  each denote a kaon or a pion, are searched for [18]. So far only the resonant decay  $B^0 \rightarrow p\bar{p}K^{*0}$  has been seen by the BaBar [19] and Belle [20] Collaborations while the other decays of this family are still unobserved. The  $B_{(s)}^0$  candidates are formed by combining four charged hadron candidates: a proton, an antiproton and an oppositely charged pair of light mesons. A boosted decision tree (BDT) classifier [21,22] is used to reduce the combinatorial background and PID requirements are used to distinguish between the different final states. To reject contributions from intermediate charm states, candidates with  $h^+h'^-$  invariant mass consistent with a  $D^0$  meson or  $ph^+h'^-$  invariant mass consistent with a  $\Lambda_c^+$  baryon are removed. The contributions from charmonium resonances decaying to  $p\bar{p}$  final state are removed by requiring the invariant mass of the  $p\bar{p}$  pair to be less than  $2850 \text{ MeV}/c^2$ . For the normalisation mode, namely the  $B^0 \rightarrow (J/\psi \rightarrow p\bar{p})(K^{*0} \rightarrow K^+\pi^-)$  decay, the vetoes to remove the charm components are not applied, using instead a cut around the  $J/\psi$  and  $K^{*0}$  masses. The signal yields are extracted by a simultaneous unbinned extended maximum likelihood fit to the three  $p\bar{p}h^+h'^-$  final states while the yield of the normalisation mode is extracted by an unbinned extended maximum likelihood fit to the  $p\bar{p}K^\pm\pi^\mp$ ,  $p\bar{p}$  and  $K^\pm\pi^\mp$  invariant masses. The result of the fit to the  $p\bar{p}K^+K^-$  invariant mass is shown in fig. 2 together with the efficiency corrected and background subtracted [17]  $p\bar{p}$  mass distribution for the  $B^0 \rightarrow p\bar{p}K^\pm\pi^\mp$  decay where the threshold enhancement is clearly visible. The decays  $B_s^0 \rightarrow p\bar{p}K^+K^-$ ,  $B_s^0 \rightarrow p\bar{p}K^\pm\pi^\mp$ ,  $B^0 \rightarrow p\bar{p}K^\pm\pi^\mp$  and  $B^0 \rightarrow p\bar{p}\pi^+\pi^-$  are observed with a significance greater than  $5\sigma$ ; evidence at  $4.1\sigma$  is found for the  $B^0 \rightarrow p\bar{p}K^+K^-$  decay and an upper limit is set on the branching fraction for  $B_s^0 \rightarrow p\bar{p}\pi^+\pi^-$ :  $\mathcal{B}(B_s^0 \rightarrow p\bar{p}\pi^+\pi^-) < 6.6 \times 10^{-7}$  at 90% confidence level.

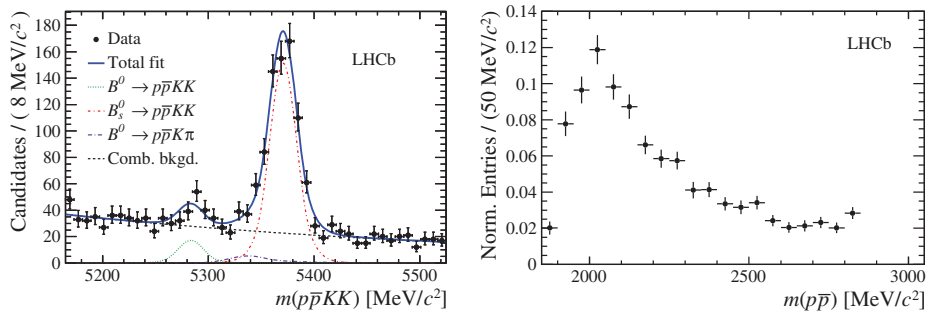


Fig. 2. – (Left) Result of the fit in the  $p\bar{p}K^+K^-$  mass spectrum. (Right) Efficiency corrected and background subtracted [17]  $p\bar{p}$  mass distribution for the  $B^0 \rightarrow p\bar{p}K^\pm\pi^\mp$  decay. Reproduced from [18].

The branching fractions of the  $B_{(s)}^0 \rightarrow p\bar{p}h^+h'^-$  modes are measured to be

$$\begin{aligned}
 \mathcal{B}(B^0 \rightarrow p\bar{p}K^+K^-) &= (0.113 \pm 0.028 \pm 0.011 \pm 0.008) \times 10^{-6}, \\
 \mathcal{B}(B_s^0 \rightarrow p\bar{p}K^+K^-) &= (4.2 \pm 0.3 \pm 0.2 \pm 0.3 \pm 0.2) \times 10^{-6}, \\
 \mathcal{B}(B^0 \rightarrow p\bar{p}K^\pm\pi^\mp) &= (5.9 \pm 0.3 \pm 0.3 \pm 0.4) \times 10^{-6}, \\
 \mathcal{B}(B_s^0 \rightarrow p\bar{p}K^\pm\pi^\mp) &= (1.30 \pm 0.21 \pm 0.11 \pm 0.09 \pm 0.08) \times 10^{-6}, \\
 \mathcal{B}(B^0 \rightarrow p\bar{p}\pi^+\pi^-) &= (2.7 \pm 0.1 \pm 0.1 \pm 0.2) \times 10^{-6}, \\
 \mathcal{B}(B_s^0 \rightarrow p\bar{p}\pi^+\pi^-) &= (0.41 \pm 0.17 \pm 0.04 \pm 0.03 \pm 0.02) \times 10^{-6},
 \end{aligned}$$

where the first uncertainties are statistical, the second systematic, the third come from the uncertainty on the branching fraction of the normalisation mode and the fourth, when present, from the uncertainty on  $f_d/f_s$ .

### 3. – CP violation in b decays

**3.1. Time-dependent CP violation in the  $B^0 \rightarrow \pi^+\pi^-$  and  $B_s^0 \rightarrow K^+K^-$  decays.** – Assuming  $CPT$  invariance, the  $CP$  asymmetries as a function of time between  $B_{(s)}^0$  and  $\bar{B}_{(s)}^0$  mesons decaying to a  $CP$  eigenstate  $f$  is given by

$$\mathcal{A}(t) = \frac{\Gamma_{\bar{B}_{(s)}^0 \rightarrow f}(t) - \Gamma_{B_{(s)}^0 \rightarrow f}(t)}{\Gamma_{\bar{B}_{(s)}^0 \rightarrow f}(t) + \Gamma_{B_{(s)}^0 \rightarrow f}(t)} = \frac{-C_f \cos(\Delta m_{d,s}t) + S_f \sin(\Delta m_{d,s}t)}{\cosh\left(\frac{\Delta\Gamma_{d,s}t}{2}\right) + A_f^{\Delta\Gamma} \sinh\left(\frac{\Delta\Gamma_{d,s}t}{2}\right)},$$

where  $\Delta m_{d,s}$  and  $\Delta\Gamma_{d,s}$  are the mass and width differences of the mass eigenstates in the  $B_{(s)}^0 - \bar{B}_{(s)}^0$  system. The quantities  $C_f$ ,  $S_f$  and  $A_f^{\Delta\Gamma}$  parameterise  $CP$  violation in the decay and in the interference between mixing and decay [15] and satisfy the condition  $|C_f|^2 + |S_f|^2 + |A_f^{\Delta\Gamma}|^2 = 1$ . A rich set of physics processes contribute to the decays  $B^0 \rightarrow \pi^+\pi^-$  and  $B_s^0 \rightarrow K^+K^-$  (interference between tree and penguin transitions, neutral  $B$  mixing and possible new physics contributing to the loop transitions) and the time-dependent  $CP$  violation is sensitive to the phases  $\gamma$  and  $-2\beta_s$  of the CKM

matrix [23]. The parameters  $C_{\pi^+\pi^-}$  and  $S_{\pi^+\pi^-}$  are well constrained by the  $B$ -factories and by LHCb while the parameters  $C_{K^+K^-}$  and  $S_{K^+K^-}$  have been measured only by LHCb using  $1\text{ fb}^{-1}$  of integrated luminosity [24] and no measurement for  $A_{K^+K^-}^{\Delta\Gamma}$  has been done yet. A new measurement is done using the full Run I dataset [25]. A BDT is used to suppress the combinatorial background while a PID selection is used to reduce contamination from other  $B \rightarrow h^+h'^-$  modes to  $\sim 10\%$  of the signal. The  $CP$ -violating parameters are determined from a simultaneous unbinned maximum likelihood fit to the  $\pi^+\pi^-$ ,  $K^+K^-$  and  $K^+\pi^-$  final states. Four variables are included in the fit: the invariant mass, the decay time, the per-event mistag probability and the per-event decay time error. It is essential to take into account the per-event mistag probability and the per-event decay time error as they reduce the amplitude of the time-dependent  $CP$  asymmetries. To determine the initial flavour of the signal  $B$  meson the so-called opposite-side taggers [26] are used and are calibrated using the  $B^0 \rightarrow K^+\pi^-$  decay. The per-event decay time resolution is determined from the decay time error computed during the reconstruction and it is calibrated with the decays  $B^0 \rightarrow D^-\pi^+$  and  $B_s^0 \rightarrow D_s^-\pi^+$ . The production asymmetry is determined from the decays  $B^0 \rightarrow K^+\pi^-$  and  $B_s^0 \rightarrow K^-\pi^+$ . The results of the fit are

$$\begin{aligned} C_{K^+K^-} &= 0.24 \pm 0.06 \pm 0.02, & C_{\pi^+\pi^-} &= -0.24 \pm 0.07 \pm 0.01, \\ S_{K^+K^-} &= 0.22 \pm 0.06 \pm 0.02, & S_{\pi^+\pi^-} &= -0.68 \pm 0.06 \pm 0.01, \\ A_{K^+K^-}^{\Delta\Gamma} &= -0.75 \pm 0.07 \pm 0.11, \end{aligned}$$

where the first uncertainties are statistical and the second systematic. These results are in agreement with ref. [24] and approximately twice more precise, they also constitute the most precise measurement of  $S_{\pi^+\pi^-}$  performed by a single experiment. Neglecting the small correlations between  $C_{K^+K^-}$ ,  $S_{K^+K^-}$  and  $A_{K^+K^-}^{\Delta\Gamma}$  and dividing the central values of the measurements by the sum in quadrature of the statistical and systematic uncertainties, the significance for  $(C_{K^+K^-}, S_{K^+K^-}, A_{K^+K^-}^{\Delta\Gamma})$  to differ from  $(0, 0, 1)$  is determined to be  $4.7\sigma$ ; that of  $(C_{K^+K^-}, S_{K^+K^-})$  to differ from  $(0, 0)$  is found to be  $4.6\sigma$  and those of  $C_{K^+K^-}$  and  $S_{K^+K^-}$  to differ from 0 are found to be  $3.6\sigma$  and  $3.3\sigma$  respectively. This constitute thus the first evidence of  $CP$  violation in the  $B_s^0 \rightarrow K^+K^-$  decay.

**3.2. Evidence for  $CP$  violation in  $\Lambda_b^0 \rightarrow p\pi^-\pi^+\pi^-$ .** – Despite being predicted by the Standard Model,  $CP$  violation in baryons has not been observed yet. The decay  $\Lambda_b^0 \rightarrow p\pi^-\pi^+\pi^-$  is a good candidate for an observation as tree and penguin diagrams contributing to this decay have similar magnitude. Moreover local  $CP$  violation can be larger than the global one, integrated over the phase space [27]. Scalar triple products of final-state particle momenta in the  $\Lambda_b^0$  centre-of-mass frame are studied to search for  $P$ - and  $CP$ -violating effects [28] in the decays  $\Lambda_b^0 \rightarrow p\pi^-\pi^+\pi^-$  and  $\Lambda_b^0 \rightarrow p\pi^-K^+K^-$  using as control mode the  $\Lambda_b^0 \rightarrow (\Lambda_c^+ \rightarrow pK^-\pi^+)\pi^-$  decay [29]. The signal yields of  $\Lambda_b^0 \rightarrow p\pi^-\pi^+\pi^-$  and  $\Lambda_b^0 \rightarrow p\pi^-K^+K^-$  are extracted using an unbinned extended maximum likelihood fits to the  $p\pi^-\pi^+\pi^-$  and  $p\pi^-K^+K^-$  invariant mass distributions and are found to be  $6646 \pm 105$  and  $1030 \pm 56$ , respectively. This is the first observation of these decay modes. Signal candidates are split in four categories according to  $\Lambda_b^0$  or  $\bar{\Lambda}_b^0$  flavour and to the sign of the triple product. This allows to compute the global  $P$  and  $CP$  violation. Moreover, to evaluate the local  $P$  and  $CP$  violation two different binning schemes are used for  $\Lambda_b^0 \rightarrow p\pi^-\pi^+\pi^-$ : scheme A that divides the phase space in twelve regions dominated by two-body resonances ( $\rho^0(770)$ ,  $\Delta^{++}$ ,  $N^*$ ), and scheme B that uses

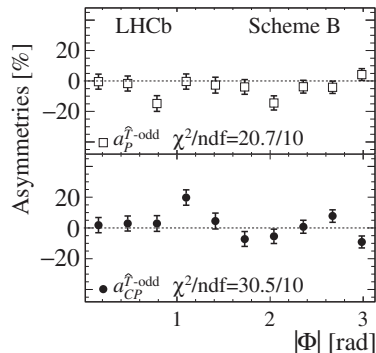


Fig. 3. – The results of the fit in each region of binning scheme B; The asymmetries sensitive to  $P$  and  $CP$  violation are represented by open boxes and filled circles respectively. The error bars indicate the total uncertainties. The values of the  $\chi^2/\text{ndf}$  are quoted for the  $P$ - and  $CP$ -conserving hypotheses. Reproduced from [29].

ten uniform bins in the angle  $\Phi$  defined as the angle between the decay plane of the proton and the  $\pi^-$  with the larger momentum and the decay plane of the other two pions. Due to its limited yield the phase space of  $\Lambda_b^0 \rightarrow p\pi^-K^+K^-$  is divided in only two bins in the  $pK^-$  invariant mass. The measurements of asymmetries in the entire phase space do not show any evidence of  $P$  or  $CP$  violation. The results are consistent with local  $CP$  symmetry for the  $\Lambda_b^0 \rightarrow p\pi^-K^+K^-$  decay, but evidence for  $CP$  violation at the  $3.3\sigma$  level is found in the  $\Lambda_b^0 \rightarrow p\pi^-\pi^+\pi^-$  decay. Results are consistent with  $P$  symmetry. Figure 3 shows the value of these asymmetries for scheme B.

#### 4. – Rare $B$ decays

4.1. *Search for the  $B_s^0 \rightarrow \eta'\phi$  decay.* – The decay  $B_s^0 \rightarrow \eta'\phi$  proceeds via a  $b \rightarrow s\bar{s}s$  penguin transition like  $B_s^0 \rightarrow \phi\phi$  and  $B_s^0 \rightarrow \eta'\eta'$ . This decay has not been observed yet and theoretical predictions for its branching fraction cover a wide range, going from  $0.05_{-0.19}^{+1.18} \times 10^{-6}$  [30] to  $20.0_{-9.1}^{+16.3} \times 10^{-6}$  [31] (for the other predictions see references in ref. [32]) and have large uncertainties due to limited knowledge on form factors, penguin contributions,  $\omega$ - $\phi$  mixing angle and  $s$ -quark mass. A search for this decay is performed using as normalisation mode  $B^+ \rightarrow \eta'K^+$ . The  $\eta'$  candidates are reconstructed as  $\eta' \rightarrow \pi^+\pi^-\gamma$  and the  $\phi$  candidates from a pair of oppositely charged kaons. In order to avoid any bias, the signal region in the  $B_s^0$ -candidate invariant mass spectrum was not inspected until the candidate selection and the fit model were finalised. An unbinned extended maximum likelihood fit is performed simultaneously to the  $\eta'K^+K^-$  and  $\pi^+\pi^-\gamma$  invariant masses to extract the signal yield. The fit produces no indication of the signal (with a yield of  $-3.2_{-3.8}^{+5.0}$ ) and an upper limit on the branching fraction is set,  $\mathcal{B}(B_s^0 \rightarrow \eta'\phi) < 0.82(1.01) \times 10^{-6}$  at 90%(95%) confidence level. This value is significantly smaller than most of the central values of the theoretical predictions available.

4.2. *Observation of the  $B^0 \rightarrow K^+K^-$  decay.* – The decays  $B^0 \rightarrow K^+K^-$  and  $B_s^0 \rightarrow \pi^+\pi^-$  proceed via weak annihilation transitions as all the quarks in the final state are different from those in the initial one. For this reason they are highly suppressed but their branching fraction may be enhanced by rescattering effects. A precise knowledge of the branching fraction of these two decays is thus essential to understand the QCD dynamics

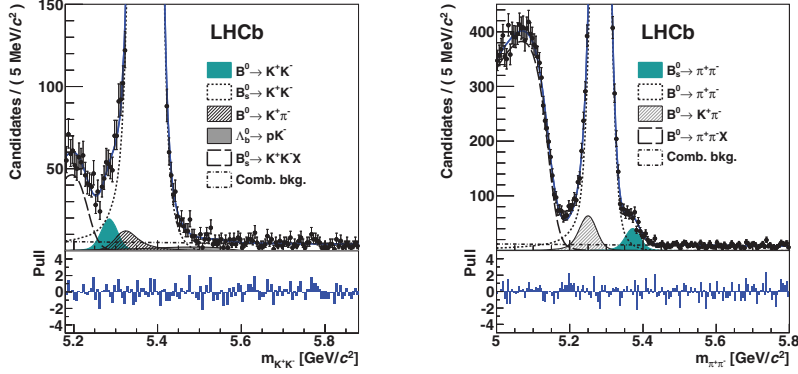


Fig. 4. – Result of the fit in the (left)  $K^+K^-$  and (right)  $\pi^+\pi^-$  mass spectra. The continuous blue curves represent the results of the best fits to the data points. The most relevant contributions to the invariant mass spectra are shown as indicated in the legends. The vertical scales are chosen to magnify the relevant signal regions. The bin-by-bin differences between the fits and the data, in units of standard deviations, are also shown. Reproduced from [34].

in the two-body decays of  $B_{(s)}^0$  to pions and kaons. The decay  $B_s^0 \rightarrow \pi^+\pi^-$  has already been observed by LHCb using  $0.37 \text{ fb}^{-1}$  of integrated luminosity [33] while  $B^0 \rightarrow K^+K^-$  has not been observed yet. A search for the  $B^0 \rightarrow K^+K^-$  and  $B_s^0 \rightarrow \pi^+\pi^-$  decays is performed using as normalisation mode  $B \rightarrow K^+\pi^-$  [34]. A BDT allows to reduce the combinatorial background while a PID selection is used to discriminate between the different final states. The signal region in the  $B_{(s)}^0$ -candidate invariant mass spectra was not inspected until the candidate selection and the fit model were finalised, in order to avoid any bias. The yields of the signal decays and of the normalisation mode have been extracted with a binned extended maximum likelihood fit performed simultaneously to the two-body invariant mass of several mutually exclusive subsamples ( $K^+\pi^-$ ,  $pK^-$ ,  $p\pi^-$ ,  $\pi^+\pi^-$  and  $K^+K^-$ ). The result of the fit in the  $K^+K^-$  and  $\pi^+\pi^-$  mass spectra is shown in fig. 4. The decay  $B^0 \rightarrow K^+K^-$  is observed at  $5.8\sigma$  and the two measured branching fractions are

$$\begin{aligned} \mathcal{B}(B^0 \rightarrow K^+K^-) &= (7.80 \pm 1.27 \pm 0.81 \pm 0.21) \times 10^{-8}, \\ \mathcal{B}(B_s^0 \rightarrow \pi^+\pi^-) &= (6.91 \pm 0.54 \pm 0.63 \pm 0.19 \pm 0.40) \times 10^{-7}, \end{aligned}$$

where the first uncertainties are statistical, the second systematic, the third come from the uncertainty on the branching fraction of the normalisation mode and the fourth from the uncertainty on  $f_d/f_s$ . This result is in agreement within uncertainties with the prediction of perturbative QCD [35] while the prediction from QCD factorisation [31] is in agreement for  $\mathcal{B}(B^0 \rightarrow K^+K^-)$  but it is significantly smaller for  $\mathcal{B}(B_s^0 \rightarrow \pi^+\pi^-)$ .

## 5. – Conclusions

Six recent LHCb results in the field of charmless  $b$ -hadron decays have been presented: the first observation of a  $B_s^0$  baryon decay, the first observation of three new  $B_{(s)}^0 \rightarrow p\bar{p}h^+h'^-$  decay modes and the evidence of a fourth one, the first observation of the decay  $B^0 \rightarrow K^+K^-$  – the rarest hadronic  $B$  decay ever observed – and the first evidence of  $CP$  violation in baryon decays and in the  $B_s^0 \rightarrow K^+K^-$  decay.



\* \* \*

The author wishes to thank the Regional Authority of Aosta Valley for the Young Scientists Fellowship to attend the XXXI Rencontres de Physique de la Vallée d'Aoste.

## REFERENCES

- [1] ALVES JR. A. A. *et al.*, *JINST*, **3** (2008) S08005.
- [2] AAIJ R. *et al.*, *Int. J. Mod. Phys. A*, **30** (2015) 1530022.
- [3] ABE K. *et al.*, *Phys. Rev. Lett.*, **88** (2002) 181803.
- [4] BEVAN A. J. *et al.*, *Eur. Phys. J. C*, **74** (2014) 3026.
- [5] AAIJ R. *et al.*, *Phys. Rev. Lett.*, **113** (2014) 152003.
- [6] AAIJ R. *et al.*, *Phys. Rev. Lett.*, **113** (2014) 141801.
- [7] AAIJ R. *et al.*, *Phys. Rev. D*, **88** (2013) 052015.
- [8] AAIJ R. *et al.*, *JHEP*, **10** (2013) 005.
- [9] AAIJ R. *et al.*, *JHEP*, **04** (2017) 162, arXiv:1611.07805.
- [10] ABE K. *et al.*, *Phys. Rev. Lett.*, **89** (2002) 151802.
- [11] WANG M. Z. *et al.*, *Phys. Lett. B*, **617** (2005) 141.
- [12] LEE Y. J. *et al.*, *Phys. Rev. Lett.*, **93** (2004) 211801.
- [13] AAIJ R. *et al.*, *Phys. Rev. Lett.*, **119** (2017) 041802, arXiv:1704.07908.
- [14] HULSBERGEN W. D., *Nucl. Instrum. Methods A*, **552** (2005) 566.
- [15] PATRIGNANI C. *et al.*, *Chin. Phys. C*, **40** (2016) 100001.
- [16] RUMELHART D. E., HINTON G. E. and WILLIAMS R. J., *Parallel Distributed Processing: Explorations in the Microstructure of Cognition* Vol. **1** (MIT, Cambridge, USA) 1986.
- [17] PIVK M. and LE DIBERDER F. R., *Nucl. Instrum. Methods A*, **555** (2005) 356.
- [18] AAIJ R. *et al.*, *Phys. Rev. D*, **96** (2017) 051103, arXiv:1704.08497.
- [19] AUBERT B. *et al.*, *Phys. Rev. D*, **76** (2007) 092004.
- [20] CHEN J. H. *et al.*, *Phys. Rev. Lett.*, **100** (2008) 251801.
- [21] BREIMAN L., FRIEDMAN J. H., OLSEN R. A. and STONE C. J., *Classification and regression trees* (Wadsworth international group, Belmont, California, USA) 1984.
- [22] FREUND Y. and SCHAPIRE R. E., *J. Comput. Syst. Sci.*, **55** (1997) 119.
- [23] AAIJ R. *et al.*, *Phys. Lett. B*, **739** (2015) 1.
- [24] AAIJ R. *et al.*, *JHEP*, **10** (2013) 183.
- [25] LHCb COLLABORATION, *Measurement of time-dependent CP violating asymmetries in  $B^0 \rightarrow \pi^+\pi^-$  and  $B_s^0 \rightarrow K^+K^-$  decays at LHCb*, LHCb-CONF-2016-018 (2016).
- [26] AAIJ R. *et al.*, *Eur. Phys. J. C*, **72** (2012) 2022.
- [27] HSIAO Y. K. and GENG C. Q., *Phys. Rev. D*, **91** (2015) 116007.
- [28] DURIEUX G. and GROSSMAN Y., *Phys. Rev. D*, **92** (2015) 076013.
- [29] AAIJ R. *et al.*, *Nat. Phys.*, **13** (2017) 391.
- [30] BENEKE M. and NEUBERT M., *Nucl. Phys. B*, **675** (2003) 333.
- [31] CHENG H.-Y. and CHUA C.-K., *Phys. Rev. D*, **80** (2009) 114026.
- [32] AAIJ R. *et al.*, *JHEP*, **05** (2017) 158, arXiv:1612.08110.
- [33] AAIJ R. *et al.*, *JHEP*, **10** (2012) 037.
- [34] AAIJ R. *et al.*, *Phys. Rev. Lett.*, **118** (2017) 081801.
- [35] XIAO Z.-J., WANG W.-F. and FAN Y.-Y., *Phys. Rev. D*, **85** (2012) 094003.